ESA Climate Change Initiative Plus (CCI+)

End-to-end ECV Uncertainty Budget: University of Leicester full-physics XCO₂ retrieval algorithm for CO2_TAN_OCFP v1

for the Essential Climate Variable (ECV)

Greenhouse Gases (GHG)

for data set

Climate Research Data Package No. 5

(CRDP#5)

Version 1, revision 1

20th December 2019

Written by
Dongxu Yang and Hartmut Boesch
Department of Physics and Astronomy and National Centre for Earth Observation
University of Leicester
Leicester
United Kingdom

Document history:

Version	Revision	Date	Description/Comments
1	0	26/10/2019	First version of CO2_TAN_OCFP E3UB document
1	1	20/12/2019	Corrections in response to comments by ESA

ESA Climate Change Initiative Plus (CCI+)
End-to-end ECV Uncertainty Budget (E3UB)
CO2_TAN_OCFP v1
for the Essential Climate Variable (ECV)
Greenhouse Gases (GHG)

Page 3

Version 1
20th December
2019

Contents

1. List of tables and figures

1.1 List of tables

1.2 List of figures

	ESA Climate Change Initiative Plus (CCI+)	Page 6
	End-to-end ECV Uncertainty Budget (E3UB)	
	CO2_TAN_OCFP v1	Version 1
	for the Essential Climate Variable (ECV)	20th December
	Greenhouse Gases (GHG)	2019

2. Executive Summary

This report provides a summary of error characterisation work for the University of Leicester OCFP/TanSat v1 XCO_2 product (CO2_TAN_OCFP v1) spanning March 2017 to May 2018. The product is validated with co-located Total Column Carbon Observing Network (TCCON) Fourier Transform Spectrometer (FTS) measurements. High overall correlation between matched soundings of 0.82 is found. Systematic and random errors are 0.19 ppm and 1.78 ppm respectively. Stability has not been assessed due to the short time series. Tests are made for correlations with influential external retrieval parameters.

3. Introduction

3.1 Purpose of document

This E3UB provides an overview of random and systematic errors affecting the UoL CO2_TAN_OCFP v1 TanSat XCO_2 retrieval submitted for the European Space Agency's Green House Gases Climate Change Initiative plus (ESA GHG-CCI+) Climate Research Data Package version No.5 (CRDP#5). Application of confidence limits to the retrieval are required to translate remotely sensed data presented here into model estimates of XCO_2 with a known degree of confidence, allowing detection of climate change impacts additional to the natural variability of greenhouse gases. GHG-CCI+ user requirements have placed strict measurement accuracy and precision requirements on participating GHG retrievals, enabling identification of minute changes in magnitude and sign of XCO_2 concentrations /Buchwitz et al., 2011, 2015/.

3.2 Intended audience

This document is intended for users in the modelling community applying the CO2_TAN_OCFP v1 product for CO_2 inversions, and remote sensing experts interested in atmospheric soundings of XCO_2. Work presented here should give users a better understanding of error implicit to this GHG-CCI+ product.

3.3 Error term definitions

Error terms used in this report are defined to maintain consistency with other CCI (CCI+) user group error terms recommended at the 2014 CCI co-location meeting. Following the descriptions of /Buchwitz et al., 2015/ and /Wagner et al., 2012/:

Error	Difference between measured values and reality (residual of a measurement's accuracy).
Uncertainty	Degree of confidence in the range of a measured value's truth (standard deviation).
Absolute accuracy	Proximity of remotely sensed measurement to in-situ measurement, assuming the in-situ measurement is able to provide a best estimate of observed quantity. Absolute accuracy reflects the best effort of the remote sensing system at reproducing the real-world value by incorporating all random and systematic errors affecting the retrieval.
Relative accuracy	Ratio between the instrument's calibration standard (the best possible measurement the instrument is able to make) against the instrument characteristics at the time of measurement.
Precision	Repeatability of a measurement.
Stability	Systematic error over time, with random errors largely removed by averaging of observations.
Sensitivity	Change of measurement due to instrumental and algorithmic response to physical or simulated input parameters.

	ESA Climate Change Initiative Plus (CCI+)	Page 8
	End-to-end ECV Uncertainty Budget (E3UB)	
	CO2_TAN_OCFP v1	Version 1
	for the Essential Climate Variable (ECV)	20th December
	Greenhouse Gases (GHG)	2019

4. Error sources

The majority of error is added to measurements from sources grouped into two themes – scattering of radiation into and out of the sampled light path by poorly quantified aerosol loading, cloud, surface reflectivity and meteorological parameters (temperature, pressure and humidity); and instrumental uncertainties (cross section and solar model inaccuracy, system noise and measurement resolution of instrument components) /Boesch et al., 2011/ /Connor et al., 2008/. In addition to single measurement error, issues of correlation lengths are introduced when the retrievals are used for subsequent generation of Level-3 products /Buchwitz et al., 2015/ /Chevallier et al., 2014/. The aforementioned errors can be further grouped into systematic – those which remain stable across measurement series; and random error components – noise in the system induced by unexpected and / or unaccounted for stimuli.

4.1 Systematic error

Systematic retrieval errors include algorithmic effects such as inaccuracy in the solar and radiative transfer models, essentially static for the duration of a satellite instrument's operation. The same applies to restrictions in instrument calibration accuracy, for instance modelling of the instrument line shape, which remains fixed following launch (although is modifiable when enough information on ILS degradation is accrued to model degradation effects). Viewing geometry also affects retrievals in a regular fashion by modifying the light path of sensed radiation as a function of the instrument and Sun's position, however interplay between increased path lengths and random error components such as aerosol optical depth add complications to the issue of measurement geometry. A-priori error added to XCO_2 measurements occurs when the retrieval ingests inaccurate input data from models and databases of surface reflectivity, surface pressure, vertical pressure grids, humidity profiles and a-priori CO_2 profiles.

4.2 Random error

Random errors are introduced to observations at the sensing stage of a measurement by detector noise, although to a certain extent this error parameter can be estimated as a function of detector component signal to noise ratios during instrument calibration. Far more significantly, atmospheric parameters are able to have major effects on sounding measurements by scattering light in and out of the sensed column. Errors due to unknown aerosol parameters are particularly pronounced where the scattering and absorption effects of suspended particulate matter are poorly modelled, as they inevitably will be when accounting for a tiny subset of all aerosol sizes, morphology and composition. Scattering due to high, optically thin clouds that are not screened from observation record present similar problems.

5. Methodology

5.1 TanSat mission

The Chinese Global Carbon Dioxide Monitoring Scientific Experimental Satellite (TanSat) is the first Chinese CO_2 monitoring satellite /Chen et al., 2012/, launched on 22 December 2016. TanSat provides global measurements of total column CO_2 from its NIR/SWIR bands. The mission aims are to monitor the column density of CO_2 precisely and frequently worldwide, to study the absorption and emission levels of CO_2 on a regional scale over a certain period of time, and to develop and establish advanced technologies that are essential for precise CO_2 observations /Liu et al., 2018/.

As the primary instrument onboard TanSat, Atmospheric Carbon dioxide Grating Spectrometer (ACGS) is designed to measure NIR/SWIR backscattered sunlight in the molecular oxygen (O_2) A band (0.76 μm) and two CO_2 bands (1.61 and 2.06 μm). Total column CO_2 is mainly determined from measurements of its absorption lines in the weak band (1.61 μm). Sunlight is significantly scattered and absorbed by air molecules and suspended particles (e.g., clouds and aerosols), which would result in serious errors in CO_2 retrievals. Consequently, more information from cloud and aerosol measurements is required for the CO_2 retrieval to correct the light path. This is acquired by the O_2 A band that provides information on altitude and total amount (optical depth) of aerosols and clouds due to almost constant and stable O_2 concentrations in the atmosphere. In comparison, the interference from water vapour absorption is relatively weak. However, the CO_2 weak band is spectrally far away from the O_2 A band, and aerosol and cloud optical properties depend on wavelength. Thus, it is also necessary to constrain this spectral variation which is one of the purposes of the strong CO_2 band. The strong CO_2 band also provides information on water vapour and temperature, which reduces impacts from uncertainties in these parameters.

The design of the optical layout of ACGS and the specifications of instrument optical parameters can be found in a previous study /Lin et al., 2017/. The footprint on the ground is 2 km × 2 km in the nadir mode with 9 footprints in each swath and a total width of the field of view (FOV) of ~18 km at nadir. The first global carbon dioxide maps produced from TanSat measurements have been produced by IAPCAS (Institute of Atmospheric Physics Carbon dioxide retrieval Algorithm for Satellite remote sensing) TanSat algorithm /Yang et al., 2018/, and then verified (~2.11 ppm of precision in 8 TCCON sites average) by TCCON Total Carbon Column Observing Network measurements /Liu et al., 2018/.

5.2 UoL CO2_TAN_OCFP v1

The UoL core CO_2 ECV product is retrieved from calibrated TanSat SWIR/NIR spectra using the UoL full-physics retrieval algorithm /Boesch et al., 2011/. The retrieval algorithm obtains XCO_2 in parts per million from a simultaneous fit of the near-infrared O_2 A band spectrum at 0.76 μm and the CO_2 band at 1.61 μm as measured by the TanSat instrument.

The retrieval algorithm employs an iterative retrieval scheme based on Bayesian optimal estimation to estimate a set of atmospheric, surface and instrument parameters from measured spectral radiances. The forward model consists of coupled radiative transfer (RT) and solar spectrum models, calculating the monochromatic spectrum of light originating from the Sun, passing through the atmosphere, reflecting from Earth's surface or scattering back from the atmosphere, exiting at the top of the atmosphere (TOA) and entering the instrument. TOA radiances are then passed to the instrument model to simulate measured radiances at the appropriate spectral resolution. The forward model employs the LIDORT RT model combined with a fast 2-orders-of-scattering vector radiative transfer code /Natraj et al., 2008/. Additionally, the code uses low-stream interpolation functionality /O'Dell, 2010/ to accelerate the RT component of the retrieval algorithm. The OCFP algorithm retrieves a CO_2 profile together with a number of additional parameters including scaling factors for H_2O and temperature profile, surface pressure, surface albedo, Solar-Induced chlorophyll Fluorescence (SIF, zero offset) and spectral slope per band, spectral shift and stretch / squeeze, extinction profiles of two aerosol profiles and one cirrus cloud profile. In addition, a wavelength dependence gain scale factor has been retrieved as an eight-orders Fourier series (See detail in Algorithm Theoretical Basis Document Version 1, Sect. 4.2.3.6) to correct continuum pattern that have been observed in spectral fitting residuals. XCO_2, error metrics and averaging kernels are calculated from the retrieved CO_2 profile following algorithm convergence. Fast cloud screening based on clear-sky surface pressure retrieved from the O_2 A band is applied in the pre-processing to reduce processing overhead on

	ESA Climate Change Initiative Plus (CCI+)	Page 10
	End-to-end ECV Uncertainty Budget (E3UB)	
	CO2_TAN_OCFP v1	Version 1
	for the Essential Climate Variable (ECV)	20th December
	Greenhouse Gases (GHG)	2019

unrequired contaminated soundings, whilst a number of post-processing quality filters /Yang et al., 2019/ are applied for removal of low-quality retrievals.

5.3 TCCON

The Total Carbon Column Observing Network (TCCON) is a global network of Fourier transform spectrometers built for the purpose of validating space-borne measurements of XCO_2 /Wunch et al., 2010/. TCCON observes these gases with a precision on mole fractions of ~0.15% for CO_2 /Toon et al., 2009/. Although providing highly accurate measurements, the sparseness of the TCCON sites presents a challenge for validation; offering precise GHG measurements for only a limited range of geographic and meteorological conditions.

Additional considerations should be made when validating with TCCON data for the differing sensitivity between TCCON and the satellite instrument, which is partly introduced by different in a-priori information used for each retrieval. Removing the influence of the retrieval a-priori, and replacing with the TCCON a-priori could allow for a fairer comparison between the two datasets, but this is not applied here. TCCON data used for error assessments come from the GGG2014 collection (available from http://tccon.ornl.gov/).

5.4 Co-location

To assess the quality of CO2_TAN_OCFP v1 observations against rigorously validated ground based TCCON values, OCFP (TanSat) soundings are matched to TCCON observations spatially and temporally. The process of matching these two data sources is referred to as co-location. Below, we detail the UoL co-location techniques, whose methodology has a bearing on subsequent error statistics.

Spatial and Temporal:
OCFP (TanSat) points are co-located with TCCON sites based on a quadrate latitude and longitude region around each TCCON site (in ±3º latitude/longitude box). Matching OCFP soundings with TCCON sites for time is a comparatively simple operation, selecting only those TCCON values whose observation time falls within ±1 hour of each OCFP sounding time. The average is taken of all TCCON points fitting these criteria for each OCFP sounding to provide the TCCON value against which to compare.

6. Error results

The co-location procedure matches 113,120 points for the CO2_TAN_OCFP v1 product. As shown in Table 1 and Figure 1, only a small mean overall bias of 0.19 ppm is found, due to the bias correction successfully accounting for most biases at the TCCON sites. An all site Pearson correlation coefficient of 0.82 details a good match of OCFP and TCCON pairs. All-site RMSE (mean of the standard deviation per site) of Δ (TCCON- OCFP) is 1.78 ppm.

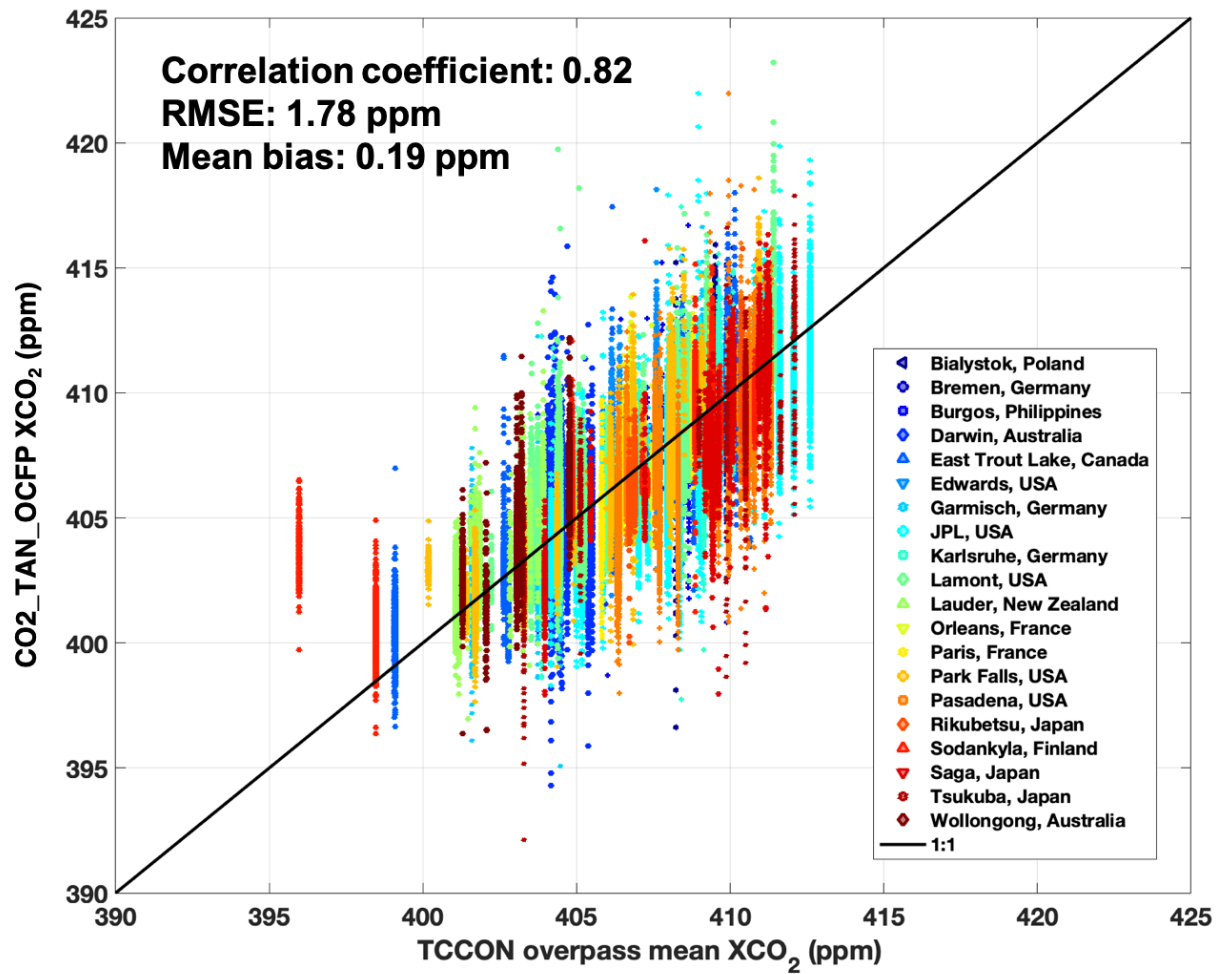| Site	Mean Δ	$\sigma\Delta$	R	n obs.
Bialystok, Poland	-0.92	1.68	0.65	3,292
Bremen, Germany	0.25	1.20	0.25	1,610
Burgos, Philippines	-0.08	2.22	0.32	310
Darwin, Australia	-0.64	2.05	-0.33	5,534
East Trout Lake, Canada	-0.17	1.26	0.90	11,923
Edwards, USA	-1.40	1.96	0.55	2,763
Garmisch, Germany	-0.32	1.67	0.67	3,704
JPL, USA	1.17	2.07	0.81	15,209
Karlsruhe, Germany	-0.29	1.62	0.84	3,089
Lamont, USA	-0.35	1.35	0.86	18,274
Lauder, New Zealand	-1.31	1.88	0.72	2,999
Orléans, France	-0.66	1.46	0.18	2,243
Paris, France	-0.08	1.40	0.76	1,503
Park Falls, USA	-0.35	1.45	0.89	13,231
Pasadena, USA	1.57	2.47	0.65	12,807
Rikubetsu, Japan	0.54	1.27	0.84	1,473
Sodankylä Finland	-1.18	2.19	0.93	6,482
Saga, Japan	0.69	1.99	0.77	4,033
Tsukuba, Japan	0.94	2.46	0.79	866
Wollongong, Australia	-1.15	1.93	0.73	1,775
Overall	0.19	1.78	0.82	113,120

Table 1. Error statistics for all TCCON sites considered for XCO_2 validation. Final row details statistics for all sites, with all co-located points used for calculations. XCO_2 units in ppm. The overall of Mean Δ and $\sigma\Delta$ is calculated by averaging of site value and r is calculated by all individual measurement. Only TCCON measurements over than 20 during each TanSat overpass has been involved in this validation.
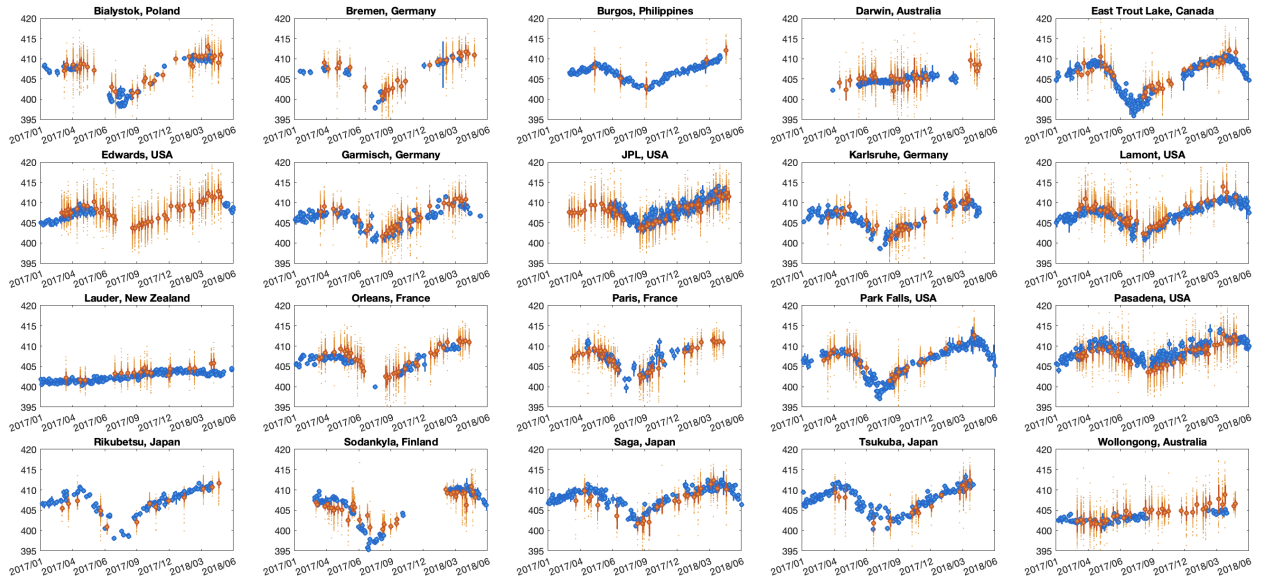
6.1 Overview statistics

Figure 2 shows per-site time series of CO2_TAN_OCFP v1 and TCCON XCO_2, with mean Δ, standard deviation of the Δ, correlation coefficient and number of observations shown in Table 1. Filtering of observations and application of a bias correction in post-processing effectively removes significant outliers and for most sites reduces the scatter of OCFP values around the TCCON mean. Note that only measurements for an overpass > 50 soundings are shown in the figure.

6.2 Systematic error

Bias correcting reduces the average TCCON–OCFP bias to 0.19 ppm for all sites (Figure 1). As detailed in Figure 2, per-site bias ranges from 1.57 ppm at Pasadena U.S.A., to -1.40 ppm at Edwards, U.S.A. The monthly mean bias for all co-located TCCON–OCFP pairs is shown in Figure 3, and the mean bias per overpass for 8 selected TCCON sites in Figure 4. We define overall systematic error as the standard deviation of inter-site TCCON–OCFP Δ, finding a value of 0.84 ppm.

	ESA Climate Change Initiative Plus (CCI+)	Page 12
	End-to-end ECV Uncertainty Budget (E3UB)	
	CO2_TAN_OCFP v1	Version 1
	for the Essential Climate Variable (ECV)	20th December
	Greenhouse Gases (GHG)	2019

Figure 1. Correlation between all 113,120 co-located CO2_TAN_OCFP and TCCON XCO$_2$ pairs coloured by site.

Figure 2. TanSat XCO_2 (CO2_TAN_OCFP v1) observations plotted with their corresponding paired TCCON mean for the overpass. Overview statistics for each site reference to Table 1.
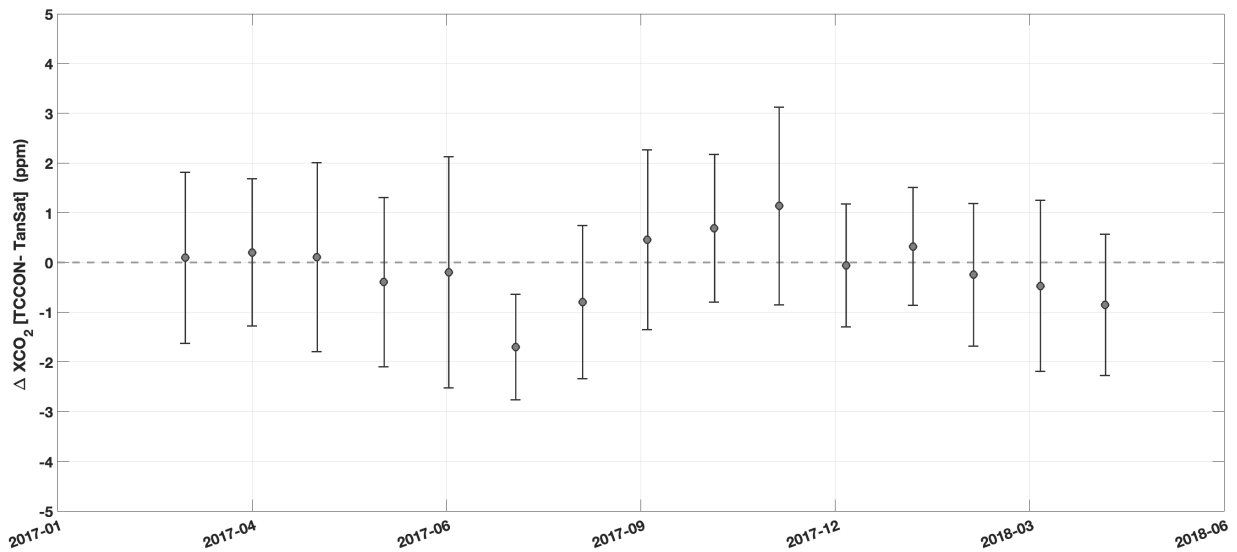
Figure 3. Monthly mean OCFP bias against TCCON (all 20 TCCON sites). Vertical error bars represent monthly standard deviation of the bias (the standard deviation of all individual bias).
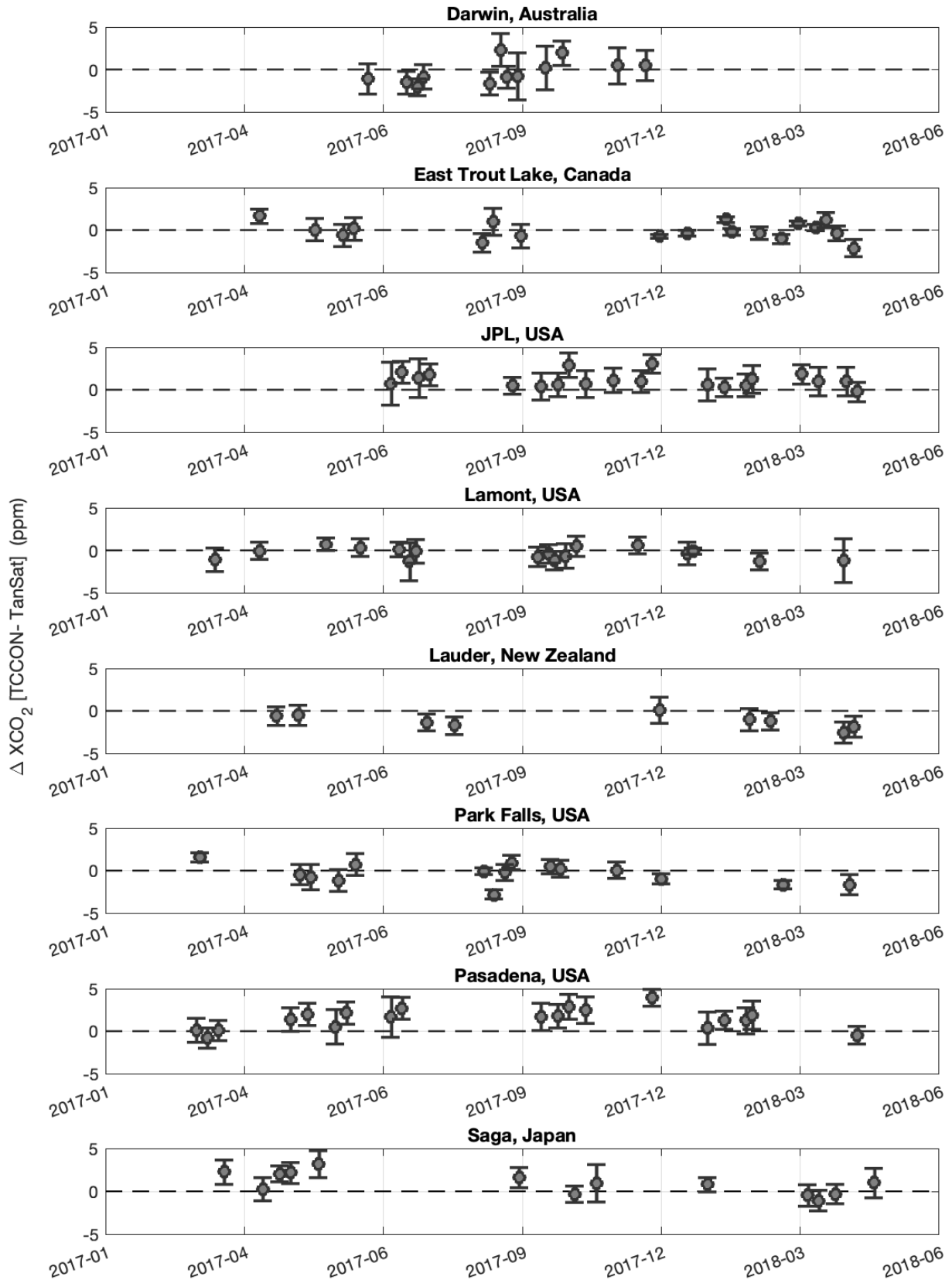
Figure 4. Overpass mean of each individual TCCON–OCFP Δ XCO$_2$ at 8 TCCON sites. The vertical error bar indicates the standard deviation of individual TCCON–OCFP Δ XCO$_2$.
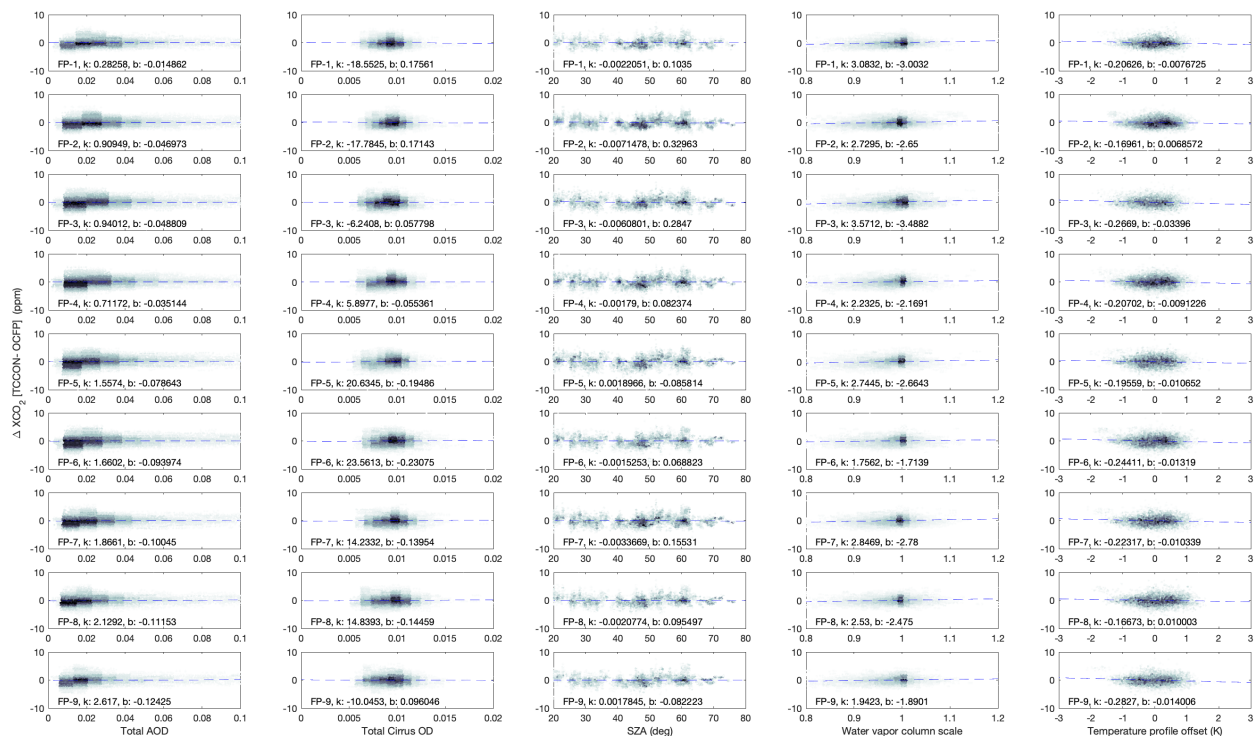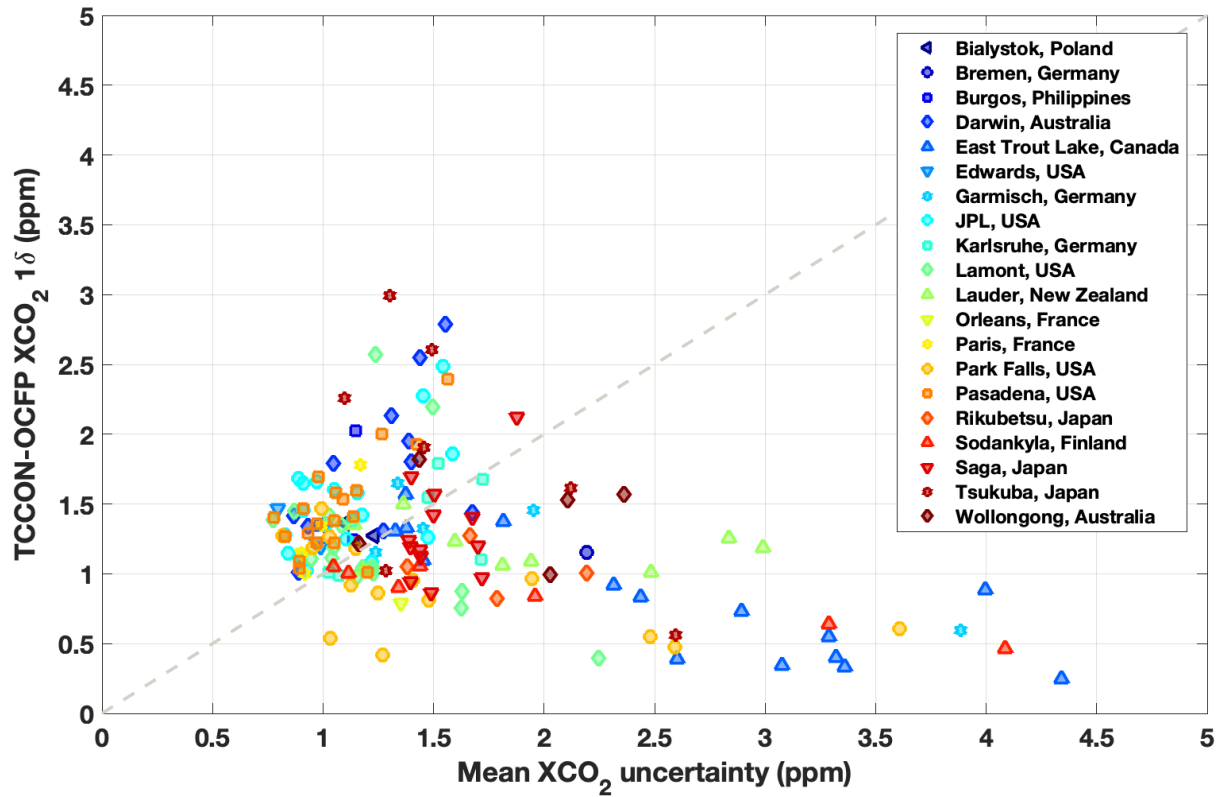
6.3 Correlations

Attempts are made to derive linear dependencies with ancillary OCFP retrieval parameters at all TCCON sites. Here the focus is on total aerosol optical depth, total cirrus optical depth, solar zenith angle (SZA), scale factor of water vapor column and offset of temperature profile. Figure 5 shows the XCO_2 bias against those parameters calculated from all overpass-paired TanSat individual sounding and mean TCCON measurement. Overall, no obvious correlated biased are found with these parameters after the bias correction is applied.

Figure 5. XCO_2 bias correlations with total aerosol optical depth, total cirrus optical depth, solar zenith angle (SZA), scale factor of water vapor column and offset of temperature profile (column from left to right) for all co-located TCCON–OCFP pairs. The rows indicate the 9 footprints from top to bottom. The linear regression parameters, slope (k) and offset (b), is shown in each sub-plot.

6.4 Random error

The random error is assessed by comparing the overpass-mean product uncertainty at each TCCON site to the standard deviation of the TCCON–OCFP pairs for each overpass and site. Figure 6 shows that the reported uncertainties are between 0.78 ppm (Lamont, U.S.A.) and 4.34 ppm (East Trout Lake, Canada). The correlation plot shows a relatively large spread of the data points which some clear outliers where the observed scatter is largely overestimated. We find that these overestimated errors are correlated with surface albedo of the CO_2 band and these very large a posterior errors appear when the surface is very dark, and subsequently the SNR is much reduced due to the low level of incident light. In these cases, the information content for CO_2 is limited so that the retrieved results remain close to the a priori values. Thus, they show a low scatter when compared to TCCON resulting in low (0.3 - 1 ppm) values in the mean TCCON–OCFP Δ standard deviation. In future versions, additional quality filters, e.g. continuum level and surface albedo, which correlate with reported a priori errors will be investigated and considered in order to improve posterior errors.

	ESA Climate Change Initiative Plus (CCI+)	Page 16
	End-to-end ECV Uncertainty Budget (E3UB)	
	CO2_TAN_OCFP v1	Version 1
	for the Essential Climate Variable (ECV)	20th December
	Greenhouse Gases (GHG)	2019

Figure 6. Correlation plot of the overpass mean estimate of the a posteriori retrieval error and TCCON–OCFP Δ standard deviation for different TCCON sites. Slope and intercept are annotated on plots.

	ESA Climate Change Initiative Plus (CCI+)	Page 17
	End-to-end ECV Uncertainty Budget (E3UB)	
	CO2_TAN_OCFP v1	Version 1
	for the Essential Climate Variable (ECV)	20th December
	Greenhouse Gases (GHG)	2019

7. Conclusions

Analysis of CO2_TAN_OCFP v1 data in conjunction with ground truth data from TCCON has given estimates of systematic and random errors, and allowed to make some inference towards correlation with external retrieval parameters. A high correlation of the compared CO2_TAN_OCFP v1 and TCCON values of 0.82 inspires confidence in the retrieval and suggests the post-processing filter and bias correction are working as intended. The random error and systematic error are 1.78 ppm and 0.19 ppm respectively. Stability has not been assessed due to the short time series.

	ESA Climate Change Initiative Plus (CCI+)	Page 18
	End-to-end ECV Uncertainty Budget (E3UB)	
	CO2_TAN_OCFP v1	Version 1
	for the Essential Climate Variable (ECV)	20th December
	Greenhouse Gases (GHG)	2019

8. Acknowledgement

9. References

/Boesch et al., 2011/ Boesch, H., Baker, D., Connor, B., Crisp, D. and Miller, C.: Global Characterization of CO_2 Column Retrievals from Shortwave-Infrared Satellite Observations of the Orbiting Carbon Observatory-2 Mission, Remote Sens., 3(12), 270–304, doi:10.3390/rs3020270, 2011.

/Buchwitz et al., 2011/ Buchwitz, M., Chevallier, F., Bergamaschi, P., Aben, I., Boesch, H., Hasekamp, O., Notholt, J. and Reuter, M.: ESA Green House Gases CCI: User Requirements Document for the GHG-CCI project of ESA's Climate Change Initiative. [online] Available from: www.esa-ghg-cci.org/?q=webfm_send/272 (Accessed 25 January 2016), 2011.

/Buchwitz et al., 2015/ Buchwitz, M., Reuter, M., Schneising, O., Boesch, H., Guerlet, S., Dils, B., Aben, I., Armante, R., Bergamaschi, P., Blumenstock, T., Bovensmann, H., Brunner, D., Buchmann, B., Burrows, J. P., Butz, A., Chédin, A., Chevallier, F., Crevoisier, C. D., Deutscher, N. M., Frankenberg, C., Hase, F., Hasekamp, O. P., Heymann, J., Kaminski, T., Laeng, A., Lichtenberg, G., De Mazière, M., Noël, S., Notholt, J., Orphal, J., Popp, C., Parker, R., Scholze, M., Sussmann, R., Stiller, G. P., Warneke, T., Zehner, C., Bril, A., Crisp, D., Griffith, D. W. T., Kuze, A., O'Dell, C., Oshchepkov, S., Sherlock, V., Suto, H., Wennberg, P., Wunch, D., Yokota, T. and Yoshida, Y.: The Greenhouse Gas Climate Change Initiative (GHG-CCI): Comparison and quality assessment of near-surface-sensitive satellite-derived CO_2 and CH_4 global data sets, Remote Sens. Environ., 162, 344–362, doi:10.1016/j.rse.2013.04.024, 2015.

/Chevallier et al., 2014/ Chevallier, F., Palmer, P. I., Feng, L., Boesch, H., O'Dell, C. W. and Bousquet, P.: Toward robust and consistent regional CO_2 flux estimates from in situ and spaceborne measurements of atmospheric CO_2, Geophys. Res. Lett., 41(3), 1065–1070, doi:10.1002/2013GL058772, 2014.

/Chen et al., 2012/ Chen., W., Zhang, Y., Yin, Z., Zheng, Y., Yan, C., Yang, Z., and Liu, Y.: The TanSat Mission: Global CO2 Observation and Monitoring, Proceedings of the 63rd IAC (International Astronautical Congress), Naples, Italy, Oct, IAC-12-B4.4.12, 1-5, 2012.

/ Connor et al., 2008/ Connor, B. J., Boesch, H., Toon, G., Sen, B., Miller, C. and Crisp, D.: Orbiting Carbon Observatory: Inverse method and prospective error analysis, J. Geophys. Res. Atmospheres, 113(D5), n/a–n/a, doi:10.1029/2006JD008336, 2008.

/Liu et al., 2018/ Liu, Y., Wang, J., Yao, L., et al., The TanSat mission: preliminary global observations, Science Bulletin, 63, 1200-1207, 2018.

/Natraj et al., 2008/ Natraj, V., Boesch, H., Spurr, R. J. D. and Yung, Y. L.: Retrieval of X_{CO2} from simulated Orbiting Carbon Observatory measurements using the fast linearized R-2OS radiative transfer model, J. Geophys. Res., 113(D11), doi:10.1029/2007JD009017, 2008.

/O'Dell et al., 2010/ O'Dell, C. W.: Acceleration of multiple-scattering, hyperspectral radiative transfer calculations via low-streams interpolation, J. Geophys. Res., 115(D10), doi:10.1029/2009JD012803, 2010.

/Toon et al., 2009/ Toon, G., Blavier, J.-F., Washenfelder, R., Wunch, D., Keppel-Aleks, G., Wennberg, P., Connor, B., Sherlock, V., Griffith, D., Deutscher, N. and Notholt, J.: Total Column Carbon Observing Network (TCCON), p. JMA3, OSA., 2009.

/Wagner et al., 2012/ Wagner, W., Dorigo, W., de Jeu, R., Parinussa, R., Scarrott, R., Kimmo, Lahoz, W., Doubková, M., Dwyer, N. and Barrett, B.: ESA Soil Moisture CCI: Comprehensive Error Characterisation Report. [online] Available from: http://www.esa-soilmoisture-cci.org/sites/default/files/documents/public/Deliverables%20-%20CCI%20SM%201/20120521_CCI_Soil_Moisture_D1.2.1_CECR_v.0.7.pdf (Accessed 25 January 2016), 2012.

	ESA Climate Change Initiative Plus (CCI+)	Page 19
	End-to-end ECV Uncertainty Budget (E3UB)	
	CO2_TAN_OCFP v1	Version 1
	for the Essential Climate Variable (ECV)	20th December
	Greenhouse Gases (GHG)	2019

/Wunch et al., 2010/ Wunch, D., Toon, G. C., Wennberg, P. O., Wofsy, S. C., Stephens, B. B., Fischer, M. L., Uchino, O., Abshire, J. B., Bernath, P., Biraud, S. C., Blavier, J.-F. L., Boone, C., Bowman, K. P., Browell, E. V., Campos, T., Connor, B. J., Daube, B. C., Deutscher, N. M., Diao, M., Elkins, J. W., Gerbig, C., Gottlieb, E., Griffith, D. W. T., Hurst, D. F., Jiménez, R., Keppel-Aleks, G., Kort, E. A., Macatangay, R., Machida, T., Matsueda, H., Moore, F., Morino, I., Park, S., Robinson, J., Roehl, C. M., Sawa, Y., Sherlock, V., Sweeney, C., Tanaka, T. and Zondlo, M. A.: Calibration of the Total Carbon Column Observing Network using aircraft profile data, Atmospheric Meas. Tech., 3(5), 1351–1362, doi:10.5194/amt-3-1351-2010, 2010.

/Yang et al., 2018/ Yang, D., Y. Liu, Z. Cai, X. Chen, L. Yao, and D. Lu, 2018: First Global Carbon Dioxide Maps Produced from TanSat Measurements. Adv. Atmos. Sci., 35(6), 621–623.

/Yang et al., 2019/ Yang, D. Boesch, H., Liu, Y., Somkuti, P., et al.: Toward high precision XCO2 retrieval on TanSat measurements: the retrieval improvement and validation against TCCON measurement. J. Geophys. Res. Atmos., 2019, in preparation.